Nanoscale

Accepted Manuscript

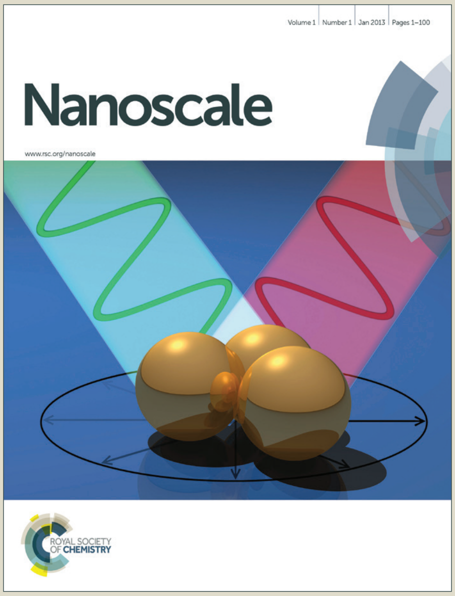

This is an *Accepted Manuscript*, which has been through the Royal Society of Chemistry peer review process and has been accepted for publication.

Accepted Manuscripts are published online shortly after acceptance, before technical editing, formatting and proof reading. Using this free service, authors can make their results available to the community, in citable form, before we publish the edited article. We will replace this *Accepted Manuscript* with the edited and formatted *Advance Article* as soon as it is available.

You can find more information about *Accepted Manuscripts* in the Information for Authors.

Please note that technical editing may introduce minor changes to the text and/or graphics, which may alter content. The journal's standard Terms & Conditions and the Ethical guidelines still apply. In no event shall the Royal Society of Chemistry be held responsible for any errors or omissions in this *Accepted Manuscript* or any consequences arising from the use of any information it contains.

ROYAL SOCIETY
OF CHEMISTRY

www.rsc.org/nanoscale

Nanoscale

Dynamic Article Links ►

Cite this: DOI: 10.1039/c0xx00000x

www.rsc.org/xxxxxx

Communication

Interaction of Nanoparticles with Lipid Membranes: a Multiscale Perspective

Costanza Montis,[a#] Daniele Maiolo,[b#] Ivano Alessandri,[b] Paolo Bergese,[b]* Debora Berti[a]*

Received (in XXX, XXX) Xth XXXXXXXXX 20XX, Accepted Xth XXXXXXXXX 20XX

DOI: 10.1039/b000000x

Freestanding lipid bilayers were challenged with 15 nm Au nanospheres either coated by a citrate layer or passivated by a protein corona. The effect of Au nanospheres on bilayer morphology, permeability and fluidity presents strong differences or similarities, depending on the observation length scale, from the colloidal to the molecular domains. These findings suggest that the interaction between nanoparticles and lipid membranes should be conveniently dealt with as a multiscale phenomenon.

Biological function is the result of a series of complex and diverse events mutually connected over several length scales. Peculiar examples are the hierarchical features of silk formation[1], cell motility[2] or gecko foot grip.[3] Although ubiquitous in Nature, this paradigm has never been exploited to describe the membrane-nanoparticle interface.

Nanoparticle (NP) size is akin to biological macromolecules, including proteins, lipids and other components of cell membranes.[4,5] In biological environments, this size matching combines with the NP high surface energy to drive a vigorous and intricate trade between the NPs and these biological entities.[6,7] It follows that the "biological identity" of NPs is ultimately determined by the size, composition, structure and time evolution of the solid-liquid interface that separates them from the biological environment, the NP-protein corona being probably the most prominent example of such an interface.[6,8]

This subject remains to date one of the primary factors that should be addressed to take medical applications of nanomaterials to the next level and to rationally address some key aspects of nanotoxicology.[9–11]

Cellular internalization and trafficking of NPs are among the most controversial subjects in the area.[12–16] Some of the underpinning mechanisms are connected to receptor-mediated pathways,[17,18] while others are lipid-mediated and determined by membrane composition,[19,20] NP size,[21] shape[22] and surface chemistry.[15] On top, unambiguous interpretation of the data obtained *in vitro* is complicated by the large variability of cellular lines and culture media.[23] Over the last years, coarse-grained and multi-scale simulations have provided useful clues,[13,24] but the complexity of the cellular membrane-NP system and the mesoscale size of the system pose difficult hurdles to theoretical routes.

The first step toward rationalization of NP-cell membrane interactions is to disentangle the physicochemical aspects from the biological ones: synthetic lipid membranes, such as giant unilamellar vesicles (GUVs), can provide a simplified, repeatable and robust experimental model for this purpose.[25,26]

GUVs were prepared through electroformation and suspended in buffer solution. They resulted 10-20 microns in size, defining a freestanding flat bilayer at the molecular length scale, which separates two aqueous regions. NP trafficking between these two regions was monitored by Confocal Laser Scanning Microscopy (CLSM) and Fluorescence Correlation Spectroscopy (FCS).[27–29]

Au spherical NPs hold promise for many biological applications, are easy to synthesize, structurally well-defined and widespread in the scientific community.[30,31] Here, we performed a comparative study between 15 nm AuNPs capped with citrate (NP@Ct) and the same NPs coated by a corona of serum proteins (NP@PC),[32] to address the two limit conditions of "naked" and "biological fluid passivated" NPs.

NP@Ct were incubated with 10% Fetal Bovine Serum (FBS) in PBS, to yield NP@PC.[33] A fluorescent protein corona of identical composition was obtained with 5-TAMRA labelled FBS (NP@LabPC). Monodisperse and negatively charged nanoparticles (hydrodynamic diameter, D_h = 28.7 nm (PDI = 0.2); ζ-potential, ζ= −28.7 ± 4.9 mV) were dispersed in 10 mM PBS, without significant aggregation in the experimental time window. The presence of the protein corona raised D_h to 87.9 nm (PDI=0.2) and ζ to −19.4 ± 3.0 mV, (full details on GUVs and on NP synthesis and characterization are provided as SI).

GUVs were challenged with 3.5 nM NP@Ct and NP@PC – a model molar concentration selected for being non toxic to cells, yet ensuring GUVs surface saturation [34] – and the bilayer-NP interaction was observed with CLSM, imaging simultaneously the bilayer fluorescence ($\lambda_{excitation}$ = 488 nm; $\lambda_{emission}$ =498 nm - 530 nm) and the light scattering from Au NPs illuminated at 633 nm ($\lambda_{acquisition}$ = 620 nm – 640 nm).[35]

Fig. 1 reports the CLSM images after two hours of equilibration, a time scale selected for ensuring the achievement of the adsorption equilibrium,[13,36,37] which evidence co-localization of lipids and NP clusters in both systems, but with marked morphological and microstructural differences.

NP@Ct (Fig. 1a÷1e) form a heterogeneous crust which disrupts large GUV regions; the molar concentration of NPs in solution is in the order of magnitude of monolayer coverage (see SI).

Cite this: DOI: 10.1039/c0xx00000x

www.rsc.org/xxxxxx

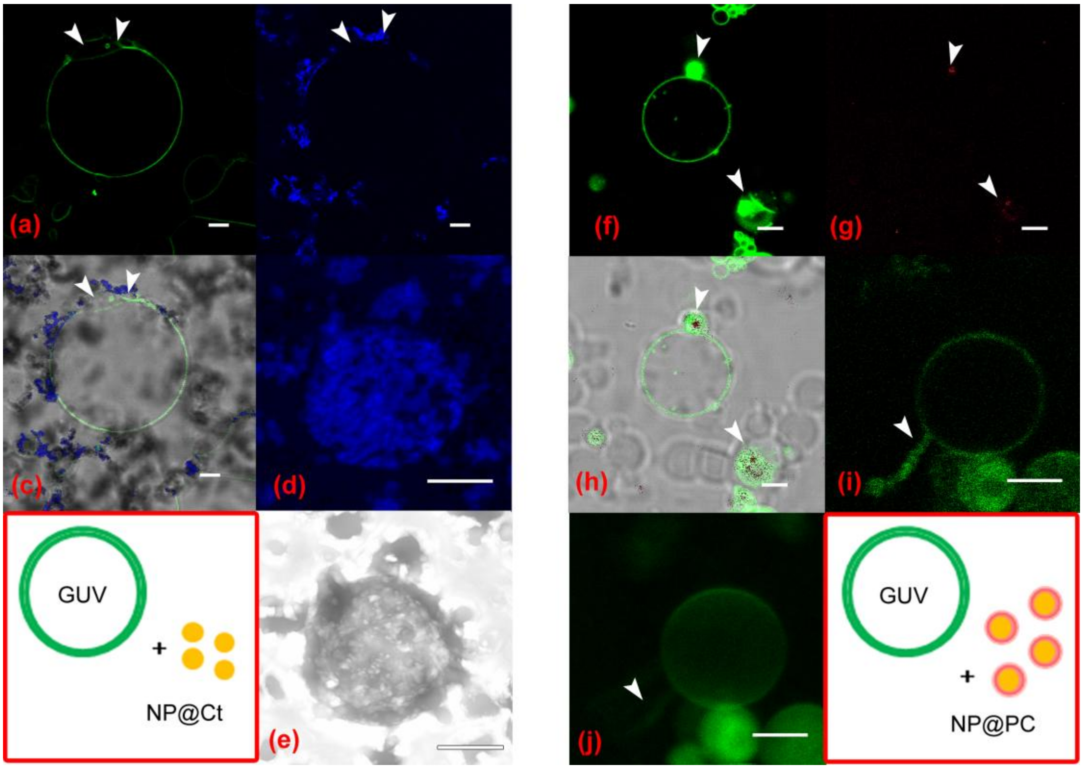

Figure 1. NP-GUV interaction from Confocal Laser Scanning Microscopy (CLSM). (a-c) NP@Ct-GUVs systems imaged through: GUVs fluorescence (a), NP@Ct scattering (b), previous images superimposed to the transmission image (c). The arrows indicate membrane alterations and poration. (d-e) 3D images of NP@Ct-GUV system (unstained GUVs) obtained by scattering **(d)** and transmission **(e). (f-h)** Images of the NP@PC-GUV systems (β-Bodipy stained GUVs), notation analogous to **(a-c).** Arrows indicate the GUVs' pearling in the presence of NPs. **(i-j)** 2D and 3D confocal images of the NP@PC-GUV systems. The arrows indicate the extrusion of nanotubes. The scale bars correspond to 5 µm.

However, the adsorption proceeds well beyond the first layer of NPs, yielding micron sized clusters, far larger than the size of the aggregates that NP@Ct form in PBS in the same time frame, (D_h ~ 300 nm (SI Fig. S4)). These observations suggest that the GUV membrane serve as an active template for the formation of this crust. We hypothesize that aspecific interactions between a NP@Ct and the lipids may not lead to complete NP coverage and therefore, in turn, the NP relieves its excess of surface energy by recruiting NPs from solution, seeding crust growth. The high surface energy characterizing citrate-coated NPs,[14,36,37] supports this hypothesis.

The formation of a protein corona occurs *via* consumption of this energy and changes the NP surface by decorating it with hydrophobic domains.[6,38] This results in a different pattern of lipid binding and self-assembly. Indeed, upon interaction with GUVs, NP@PCs form small clusters that engage a more gentle interaction with the bilayer (Figure 1f÷1j). The membrane is not disrupted, but rather reorganized into complex negative curvature structures of several microns protruding from the GUVs. Such adhesive lipid extraction, recently observed on bilayers exposed to cationic nanoparticles,[39] is here mediated by the presence of the negatively charged protein-corona.

The molecular trafficking through the GUV-NP structures was investigated with Fluorescence Correlation spectroscopy (FCS), to complete the above morphological picture with quantitative functional information, which are summarized in Figure 2. FCS allows to determine in a selected region of the sample both the diffusion coefficient (i.e. the hydrodynamic size) and the concentration of fluorescent probes, which is inversely proportional to the intercept of the FCS profiles.[40]

In a control experiment(Figure 2a), the fluorescent species (Alexa dye) is externally added to the intact GUVs without NPs. The concentration of the dye is monitored *inside* the vesicles after two hours and compared to the value recorded in the dispersing medium. A modest permeability was found in the absence of NP, with the dye concentration passing from 0 to 10% of the value recorded outside the GUVs. (see SI Fig. S6 for details)

In the presence of NPs, an increased transmembrane trafficking of dye is found, irrespectively of the NP kind (Figure 2b). The extent of this enhancement, though reproducible, was found to vary for different GUVs (Fig. S6). Interestingly, a clear difference emerges depending on the surface chemistry of the

Nanoscale

Nanoscale

Dynamic Article Links ►

Cite this: DOI: 10.1039/c0xx00000x

www.rsc.org/xxxxxx

Communication

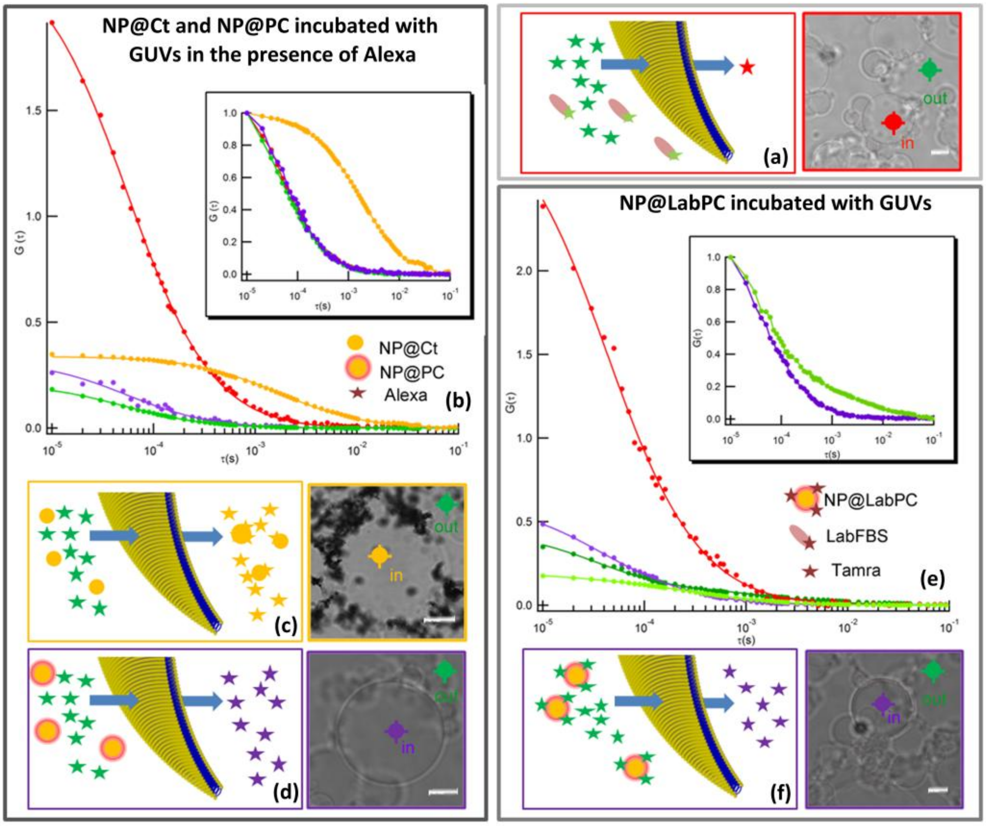

Figure 2. Bilayer permeability upon interaction with NPs. (a) Scheme of the control experiment: membrane permeability to LabFBS and Alexa, externally added to the GUVs, in the absence of NPs; **(left hand side panel)** Membrane permeability to Alexa: **(b)** representative FCS profiles of the dye monitored outside (green) and inside the GUVs in the absence of NPs (red) and in the presence of NP@Ct (yellow) and NP@PC (purple); the internal dye concentration, directly correlated with its transmembrane permeability, is clearly enhanced in the presence of NPs, as inferred from the decrease of the intercepts; **(b, inset)** the FCS curves are normalized to compare the decay times: for NP@Ct, whole NP-dye aggregates are present inside the GUVs after incubation (as sketched in the scheme **(c)**), while for NP@PC, only the diffusion of the free dye is detected,(scheme **(d)**). **(bottom right panel)** Membrane permeability to NP@LabPC: **(e)** control FCS curves monitored outside (light green) and inside (red) the GUVs in the presence of LabFBS, compared to the FCS monitored outside (dark green) and inside (purple) the GUVs' lumen after incubation with NP@LabPC; a clear enhancement of dye concentration, i.e. permeability, emerges from the comparison of intercepts; **(e, inset)** normalized FCS curves: the incubation with NP@LabPC enhances permeability of molecular species, but does not allow internalization of nanoparticle constructs, as the corresponding scheme **(f)** sketches. Moreover, while the ACFs outside GUVs are consistent with the simultaneous presence of NP@LabPC, dye molecules bound to free diffusing proteins and free dye **(see SI Fig. S7)**, inside the GUVs the decay is monomodal and due only to the free dye, as the comparison of the normalized FCS **(e, inset)** points out. Scale bars correspond to 10 µm.

NPs, as the normalized FCS profiles indicate. After exposure to NP@PC (Figure 2b, inset) it is the free Alexa dye that permeates the vesicles. Conversely, for NP@Ct, the higher decay times of the Autocorrelation Function (ACF), reveal that Alexa adsorbed on NP@Ct aggregates (Fig. S6) has crossed the GUVs. In summary, the exposure to both NP kinds increases the trafficking of external species across the bilayer, but NP@Ct cause a complete loss of the barrier function, allowing the entry of entire aggregates, while NP@PC enhance only the permeation of molecular species (Figure 2c, 2d).

To confirm this important difference, NP@PC have been prepared with FBS where the proteins are fluorescently labelled with TAMRA (LabFBS). Also in this case, it is only the residual free dye presumably adsorbed but not cross-linked to proteins, that exhibits transmembrane penetration (Figure 2e, 2f, SI Fig. S7).

Membrane leakage is one of the key events associated with cytotoxicity and more generally with the interaction of engineered nanoparticles with living systems in the environment.[11] Our results are therefore relevant both for

Cite this: DOI: 10.1039/c0xx00000x

www.rsc.org/xxxxxx

Communication

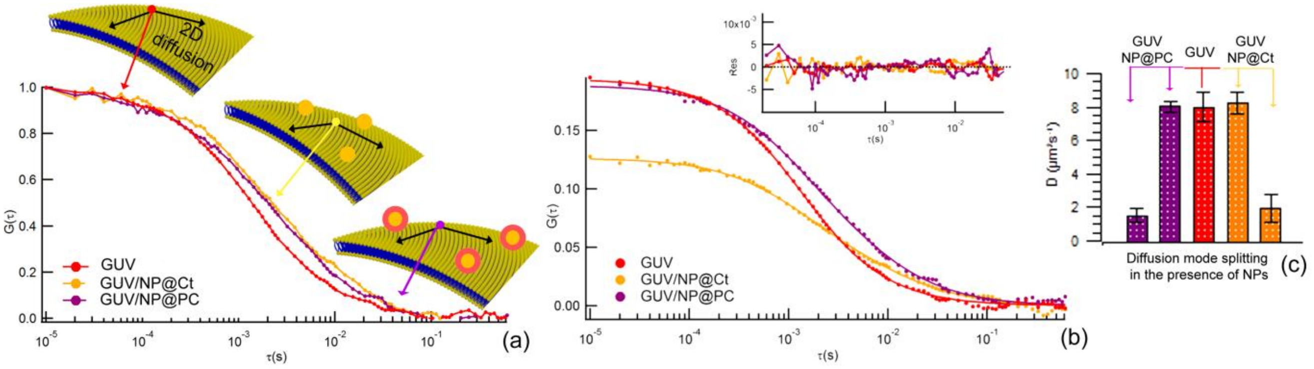

Figure 3. Diffusion of a lipid probe in the GUV bilayer after interaction with NPs. FCS measurements were performed on the GUVs' poles **(scheme a)**, with the exact position of the bilayer in the excitation volume revealed by a maximum of steady-state fluorescence intensity, as described in the SI. **(a)** Representative normalized ACFs acquired for bare GUVs (red) and on GUVs after incubation with NP@Ct (yellow) and NP@PC (purple). **(b)** Diffusion coefficient splitting in the presence of NPs, compared to monomodal 2D diffusion of bare GUVs (red). In the presence of NPs, together with unperturbed diffusion, both for GUVs-NP@Ct (yellow) and GUVs-NP@PC (purple), a bimodal diffusion emerges, with the faster diffusion coefficient consistent with unperturbed diffusion and a slower component identical within experimental uncertainty for both NP types.

nanomedicine and nanotoxicology, as the primary biological function of cell membranes is to separate distinct domains,regulate selective permeability to species through active or passive mechanisms and maintain pH and ion gradients. Increasing the resolution to the molecular level, some quantitative information were gathered by monitoring the variation of lipid translational mobility within the GUV bilayer upon interaction with NPs. In particular, we tracked the bidimensional diffusion[41] of a fluorescent lipid probe on the GUV poles via FCS, as schematized in Figure 3.

The diffusion coefficient measured in the absence of NPs, D_f = 8.0 ± 0.9 µm^{2}s^{-1}, is in agreement with the literature (Figure 3a). After incubation with NP@Ct and NP@PC, the GUVs become clearly grouped into two classes, in terms of lipid mobility. In some cases the diffusion on the poles appears completely unperturbed (see SI Fig. S8 for details). However, the majority of GUVs show on their poles the same significant shift of the ACFs towards higher decay times, related to a slowed-down diffusion, regardless if they are interacting with NP@Ct or NP@PC (Figure 3a). In both cases the lipid motion is described by a bi-modal decay (representative experimental curves, curve fit and residuals are displayed in Figure 3b), with the fast diffusive component identical to the one of unperturbed bilayers, D_f ~ 8 µm^{2}s^1, and the slow component reduced to one fourth, D_s ~ 2 µm^{2}s^{-1} (Figure 3c, Fig. S8). Therefore, the lipid motion is determined by a combination of "free" bidimensional motion and diffusion "slaved" to the NPs adsorbed on the membrane. In this picture, the interaction of NPs with the bilayer results in the formation of similarly rigidified lipid domains, where the lipid motions are slowed-down with respect to the fluid phase[42] (dark green lipids in the bilayer of Fig. 4).

The above data suggest that at the molecular level NP@Ct and NP@PC share the ability to restructure the membrane into nanoscale regions with different mobility properties. Such nanoscale membrane heterogeneities resemble lipid rafts in cells, which are involved in membrane signalling and trafficking, including lipid-mediated endocytosis.[25]

The surface chemistry underpinning this behaviour is not trivial. ζ-potentials of NP@Ct, NP@PC and GUVs are negative (150 nm POPC vesicles in PBS have ζ = – 4.9 ± 0.4 mV), implying a non obvious role of electrostatic forces in the adhesion. On the other hand hydrophobic effects[13,14,43] and other nanomachinery[44] must be taken into account.

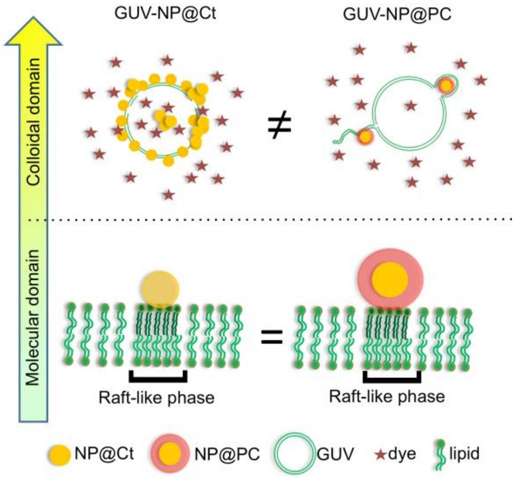

Figure 4. Cartoon sketching the multiscale nature of the interaction of citrate-coated and protein corona passivated AuNPs with a lipid bilayer at saturation concentration .

In conclusion, we found that the interaction of NP@Ct and NP@PC with lipid membranes presents similarities and differences, proceeding from the molecular to the colloidal domain and therefore can be profitably described within a multi-scale perspective as summarized in Fig. 4.

At the molecular length scale both kinds of NPs cause a similar membrane restructuring into structurally stiffened nanoscale domains. At the colloidal length scale, the NP surface identity emerges dramatically: we observe that NP@Ct crust over extended GUV domains, making the bilayer permeable to NP clusters and external fluids. Conversely, NP@PC exhibit a milder interaction with the model membranes, driving pearling and blebs that may recall macro-pynocitotic processes. In this latter case, the GUVs retain their overall integrity, and the permeability increase is lower and limited to molecular species.

Our findings set the basis for a novel multiscale approach to the investigation of the AuNP-membrane interface.

Further studies are needed to generalize this interaction pattern across the length scales to other NP/membrane systems. Such insights will contribute to advance our understanding, control and design of nanomaterials for biological applications and to elucidate one of the key processes responsible for the toxicity of engineered nanoparticles.

ACKNOWLEDGEMENTS

The authors wish to acknowledge Laura Eleonora Depero, Marco Presta, Kimberly Hamad-Schifferli, Piero Baglioni for helpful discussions and Doris Ricotta for access to laboratory equipments. This work was supported by MIUR (Ministero Italiano dell'Università e della Ricerca) through the project *Soft Matter Nanostrutturata: dall'indagine chimico-fisica allo sviluppo di applicazioni innovative*, PRIN 2010-2011 grant 2010BJ23MN.

Notes and references

[a]*Department of Chemistry "Ugo Schiff" and CSGI, University of Florence, via della Lastruccia 3, 50019 Sesto Fiorentino, Florence, Italy*
Tel:+390554573038 Fax::+3905545730384 mail: debora.berti@unifi.it; montis@csgi.unifi.it
[b] *Chemistry for Technologies Laboratory and INSTM, Department of Mechanical and Industrial Engineering, University of Brescia, via Branze 38, 25123 Brescia, Italy*
Tel:+390303715475 Fax: +390303702448
mail:paolo.bergese@ing.unibs.it; maiolo.daniele@gmail.com; ivano.alessandri@ing.unibs.it

[#]Equally contributed

*Referring authors

† Electronic Supplementary Information (ESI) available: [All the experimental details and Supplementary Figures and Tables were provided]. See DOI: 10.1039/b000000x/

1. H.-J. Jin and D. L. Kaplan, Nature, 2003, 424, 1057–1061.
2. E. A. Cavalcanti-Adam, T. Volberg, A. Micoulet, H. Kessler, B. Geiger, and J. P. Spatz, Biophysical journal, 2007, 92, 2964–74.
3. I. Gebeshuber, Nano Today, 2007, 2, 30–37.
4. P. R. Gil, G. Oberdörster, A. Elder, V. F. Puntes, and W. J. Parak, ACS nano, 2010, 4, 5527–5531.
5. B. Pelaz, S. Jaber, D. J. de Aberasturi, V. Wulf, T. Aida, J. M. de la Fuente, J. Feldmann, H. E. Gaub, L. Josephson, C. R. Kagan, N. a Kotov, L. M. Liz-Marzán, H. Mattoussi, P. Mulvaney, C. B. Murray, A. L. Rogach, P. S. Weiss, I. Willner, and W. J. Parak, ACS nano, 2012, 6, 8468–83.
6. M. P. Monopoli, C. Åberg, A. Salvati, and K. A. Dawson, Nature Nanotechnology, 2012, 7, 779–786.
7. J. C. Y. Kah, J. Chen, A. Zubieta, and K. Hamad-Schifferli, ACS nano, 2012, 6, 6730–40.
8. C. D. Walkey and W. C. W. Chan, Chemical Society reviews, 2012, 41, 2780–99.
9. B. Godin, E. Tasciotti, X. Liu, R. E. Serda, and M. Ferrari, Accounts of chemical research, 2011, 44, 979–989.
10. P. M. Valencia, O. C. Farokhzad, R. Karnik, and R. Langer, Nat Nano, 2012, 7, 623–629.
11. K. L. Chen and G. D. Bothun, Environmental science & technology, 2014, 48, 873–80.
12. A. Dubavik, E. Sezgin, V. Lesnyak, N. Gaponik, P. Schwille, and A. Eychmüller, ACS nano, 2012, 6, 2150–6.
13. R. C. Van Lehn, P. U. Atukorale, R. P. Carney, Y.-S. Yang, F. Stellacci, D. J. Irvine, and A. Alexander-Katz, Nano letters, 2013, 13, 4060-4067.
14. J. Lin, H. Zhang, Z. Chen, and Y. Zheng, ACS nano, 2010, 4, 5421–5429.
15. I. Canton and G. Battaglia, Chemical Society Reviews, 2012, 41, 2718–2739.
16. D. Bartczak, S. Nitti, T. M. Millar, and A. G. Kanaras, Nanoscale, 2012, 4, 4470–2.
17. A. Salvati, A. S. Pitek, M. P. Monopoli, K. Prapainop, F. B. Bombelli, D. R. Hristov, P. M. Kelly, C. Åberg, E. Mahon, and K. A. Dawson, Nature nanotechnology, 2013, 8, 137–143.
18. J. Rauch, W. Kolch, S. Laurent, and M. Mahmoudi, Chemical reviews, 2013, 113, 3391–406.
19. M. Mahmoudi, J. Meng, X. Xue, X. J. Liang, M. Rahman, C. Pfeiffer, R. Hartmann, P. R. Gil, B. Pelaz, W. J. Parak, P. Del Pino, S. Carregal-Romero, A. G. Kanaras, and S. Tamil Selvan, Biotechnology advances, 2013, http://dx.doi.org/10.1016/j.biotechadv.2013.11.01.
20. L. Treuel, X. Jiang, and G. Nienhaus, Journal of The Royal Society Interface, 2013, 10, 1–14.
21. B. D. Chithrani, A. a Ghazani, and W. C. W. Chan, Nano letters, 2006, 6, 662–8.
22. E. C. Cho, Q. Zhang, and Y. Xia, Nature nanotechnology, 2011, 6, 385–91.
23. G. Maiorano, S. Sabella, B. Sorce, V. Brunetti, M. A. Malvindi, R. Cingolani, and P. P. Pompa, ACS nano, 2010, 4, 7481–7491.
24. T. Yue, X. Wang, F. Huang, and X. Zhang, Nanoscale, 2013.
25. D. Lingwood and K. Simons, Science , 2010, 327, 46–50.
26. C. Montis, P. Baglioni, and D. Berti, Soft Matter, 2014, 10, 39–43.
27. T. Al Kayal, E. Russo, L. Pieri, G. Caminati, D. Berti, M. Bucciantini, M. Stefani, and P. Baglioni, Soft Matter, 2012, 8, 9115–9126.
28. D. Berti, G. Caminati, and P. Baglioni, Physical Chemistry Chemical Physics, 2011, 13, 8769–8782.
29. S. Li, P. C. Hu, and N. Malmstadt, Biophysical journal, 2011, 101, 700–8.
30. K. Saha, S. S. Agasti, C. Kim, X. Li, and V. M. Rotello, Chemical reviews, 2012, 112, 2739–79.
31. A. M. Alkilany, S. E. Lohse, and C. J. Murphy, Accounts of chemical research, 2012, 46.
32. M. P. Monopoli, D. Walczyk, A. Campbell, G. Elia, I. Lynch, F. B. Bombelli, and K. A Dawson, Journal of the American Chemical Society, 2011, 133, 2525–34.
33. M. Monopoli, A. Pitek, I. Lynch, and K.A. Dawson, in Nanomaterial Interfaces in Biology SE - 11, eds. P. Bergese and K. Hamad-Schifferli, Humana Press, 2013, vol. 1025, pp. 137–155.
34. M. Chanana, P. Rivera Gil, M. a Correa-Duarte, L. M. Liz-Marzán, and W. J. Parak, Angewandte Chemie (International ed. in English), 2013, 52, 4179–83.
35. S. Klein, S. Petersen, U. Taylor, D. Rath, and S. Barcikowski, Journal of biomedical optics, 2013, 15, 036015.
36. A. Lesniak, A. Salvati, M. J. Santos-Martinez, M. W. Radomski, K. A Dawson, and C. Aberg, Journal of the American Chemical Society, 2013, 135, 1438–1444.
37. S. Zhang, A. Nelson, and P. a Beales, Langmuir : the ACS journal of surfaces and colloids, 2012, 28, 12831–7.
38. Y. Yan, K. T. Gause, M. M. J. Kamphuis, C.-S. Ang, N. M. O'Brien-Simpson, J. C. Lenzo, E. C. Reynolds, E. C. Nice, and F. Caruso, ACS nano, 2013, 7, 10960–10970.

39. Y. Yu and S. Granick, Journal of the American Chemical Society, 2009, 131, 14158–9.
40. J. Ries and P. Schwille, BioEssays : news and reviews in molecular, cellular and developmental biology, 2012, 34, 361–8.
41. L. Guo, J. Y. Har, J. Sankaran, Y. Hong, B. Kannan, and T. Wohland, ChemPhysChem, 2008, 9, 721–728.
42. B. Wang, L. Zhang, S. C. Bae, and S. Granick, Proceedings of the National Academy of Sciences, 2008, 105.
43. J. Liu, N. Lu, J. Li, Y. Weng, B. Yuan, K. Yang, and Y. Ma, Langmuir : the ACS journal of surfaces and colloids, 2013, 29, 8039–45.
44. H. de Puig, S. Federici, S. H. Baxamusa, P. Bergese, and K. Hamad-Schifferli, Small (Weinheim an der Bergstrasse, Germany), 2011, 2477–2484.